TJES
ISSN: 1813-162X
Tikrit Journal of Engineering Sciences
available online at: http://www.tj-es.com

Laminar Mixed Convective Nanofluid Flow in a Channel with Double Forward-Facing Steps: A Numerical Simulation Study

Omar A. Hussein
Mechanical Engineering Department, College of Engineering, Tikrit University, Salahuddin, Iraq
E-mail: omar_assi2008@yahoo.com

(Received 26 January 2016, Accepted 31 May 2016, Available online 31 March 2017)

Abstract

Predictions are reported for mixed convection using various types of nanofluids over forward-facing double steps in a duct. The continuity, momentum and energy equations are discretized and the simple algorithm is applied to link the pressure and flow fields inside the domain. Different types of nanoparticles Al_2O_3, CuO, SiO_2 and ZnO, with different volume fractions in range of 1-4% and different nanoparticles diameter in the range of 20 – 80nm in base fluid (water) were used. Numerical investigations are conducted using finite volume method. In this study, different parameters such as the geometrical specifications (different steps heights in the range of h_1= 0.01m-0.04m and h_2 = 0.03m-0.06m for FFS) are used. Different Reynolds numbers in the range of 50-2000 (laminar flow) are investigated to identify their effects on the heat transfer and fluid characteristics. The results indicate that SiO_2-water has the highest Nusselt number followed by Al_2O_3-water, CuO-water and ZnO-water. The Nusselt number increases as the volume fraction increases but it decreases as the nanoparticles diameter increases. The velocity magnitude increases as the density of nanofluids decreases. The recirculation region and the Nusselt number increase as the step height, Reynolds number, and the volume fraction increase.

Keywords: Mixed convection, forward-facing double steps, heat transfer enhancement, nanofluids.

تأثير جريان الحمل الحراري الطباقي المختلط للموائع النانوية داخل مجرى يحتوي على عائق مزدوج أمامي الجريان دراسة نظرية

الخلاصة

تنبؤات الحمل الحراري المختلط بأستخدام أنواع مختلفة من الموائع النانوية داخل مجرى يحتوي على عائق مزدوج أمام الجريان تم توثيقها في هذه الدراسة. اربعة أنواع من الجسيمات النانوية أستخدمت في هذه الدراسة وهي (أوكسيد الألمنيوم, أوكسيد النحاس, ثاني أكسيد السيليكون واوكسيد الزنك), تركيز الجسيمات النانوية داخل السائل كان يتراوح 1-4% وأقطار مختلفة أيضا تتراوح من 20-80 نانومتر. جرت التحقيقات العددية باستخدام طريقة الحجم المحدد. تم تطبيق معادلات الاستمرارية، والزخم والطاقة حلت باستخدام خوارزمية بسيطة لربط الضغط مع في هذه الدراسة, معايير متعددة تمت مناقشتها كالمواصفات الهندسية للمجرى (أرتفاع العوائق كانت على النحو التالي الأرتفاع الأول من 0.01م - 0.04 م والأرتفاع الثاني من 0.03م -0.06 م). دراسة تأثير عدد رينولدز بمدى يتراوح بين 50 الى 2000 (للجريان الطباقي). النتائج العددية تشير الى أن ثاني أوكسيد السيليكون-ماء لديها أعلى القيم و عدد نسلت متبوع بأوكسيد الألمنيوم-ماء, أوكسيد النحاس-ماء وأوكسيد الزنك-ماء حاز أقل عدد نسلت أزداد بزيادة تركيز الجسيمات النانوية وقطر الجسيمات داخل السائل. قيمة سرعة المائع تزداد بنقصان قيمة كثافة الموائع النانوية. تأثير عائق الجريان لم يكن واضح على الجريان داخل المجرى.

الكلمات الدالة :الحمل الحراري المختلط , مزدوج أمامي الجريان, معامل اداء انتقال الحرارة , موائع نانوية.

* Corresponding author: E-mail: omar_assi2008@yahoo.com

Introduction

Mixed convection heat transfer in forward facing double steps had been a subject of interest in many research studies. By adding increase of discretion points to the simulation, and the power of the computers devices have been improving in terms of memory and speed capability. Therefore, the implementation of numerical simulation is best than both experimental and theoretical approaches. It eschews the annoying measurements in full-scale experimental devices, and the equipment cost, and time spent for the setups constructions. So, numerical simulation were defined as the third approach which containing the two (experimental and theoretical) approaches for studying the physical laws [1].

One of the ways to enhance heat transfer in the separated regions is to employ nanofluids. Nanofluids are fluids that contain suspended nanoparticles such as metals and oxides. These nanoscale particles keep suspended in the base fluid. Thus, it does not cause an increase in pressure drop in the flow field. Past studies showed that nanofluids exhibit enhanced thermal properties, such as higher thermal conductivity and convective heat transfer coefficients compared to the base fluid; see, for example, Daungthongsuk and Wongwises[2], Wang Mujumdar[3], H.A. Mohammed et al. [4-5].

Abu-Mulaweh et al.[6-9] conducted measurements are for laminar mixed convection flow buoyancy-opposing two-dimensional flow over a vertical forward-facing step. The upstream wall of the step was an adiabatic surface, while both the downstream wall and the step were heated to a uniform temperature that was higher than temperature of the approaching air. The measurements were carried out for a step height of 0.8cm. It was observed that the laminar non-circulating flow region downstream of the step, the local Nusselt number decreased inside the recirculation flow region as the opposing buoyancy force increased.

Chiba et al.[10] conducted flow observations over a forward-facing step channel to predict the mechanism for instability of planar entry flow of the types of unstable flow patterns. Furthermore, the coalescence and appearance of the Goertler vortex pairs cause their fourth-and-back movement along the longitudinal direction of the channel, and three-dimensional lip vortices play an important role in the appearance of a pair of the Goertler vortices.

Hirofumi and Yasutaka[11] investigated turbulent flow system of a boundary layer over a forward-facing step. It was shown that pronounced counter-gradient diffusion phenomena (CDP) were especially noted on the step near from the wall. Thus, the Reynolds numbers based on the step height became (Re_h=900-3000). Therefore the detailed structure of the results of DNS can be applied to the improvement of the turbulence model and turbulent boundary layer over a forward-facing step.

Largeau and Moriniere[12] carried out measurements of aerodynamic fields and wall pressure fluctuations in separated flows over a forward facing. It was resulted that a different behavior of the flow depending on the aspect ratio l/h and δ/h for high Reynolds numbers. The Reynolds number Re_h varies from 2.88$\times 10^4$ (*h*=30mm, *Ue*=15m/s) to 12.82$\times 10^4$ (*h*=50mm, *Ue*=40m/s). It was noted that the flapping motion (low frequency) at the separation play an important role and the large scale structures in the shear layer in the generation of the wall pressure fluctuations rather than the near wall pattern bounded in the recirculation zone.

Yilmaz and Oztop[13] presented heat transfer of turbulent forced convection for double forward facing step flow. The standard $k-\varepsilon$ turbulence model was employed to get turbulence flow modeling. Effects of fluid flow step, Reynolds numbers and step lengths on heat transfer and heights were investigated. It was revealed that the heat transfer and turbulent intensity are increased with higher Re.

Very few number of research work were conducted numerically and experimentally by Dutta and Dutta[14], and Yang and Huang[15] to capture more detail of the fluid flow pattern and heat transfer phenomena in the channel with perforated baffle. Three-dimensional laminar convection flow adjacent to backward-facing step in a heated rectangular duct with a baffle mounted on the upper wall was numerically simulated by Nie et al.[16].

The problem of laminar flow over backward-facing step geometry in natural, forced, and mixed convection has been investigated extensively in the past, both numerically and experimentally by Lin et al.[17], and Hong et al.[18] and the references cited therein. On the other hand, the problem of laminar flow over a forward-facing step has received very little attention.

Chiang et al.[19] investigated developed three-dimensional channel flow expanded into the channel with an expansion ratio of 1.94. Numerical solutions for this backward-facing step problem were gotten on the basis of Reynolds numbers as high as 800, the step height, 0.942. It was observed that the rigorous mathematical foundation had facilitated the determination of the separation, continuously and separation line on the floor with the attachment line, on the roof of the channel.

The first numerical study to investigate the flow and heat transfer over a backward-facing step using nanofluids was done by Abu-Nada[20]. The Reynolds number and nanoparticles volume fraction used were in the range of ($200 \le Re \le 600$) and ($0 \le \emptyset \le 0.2$), respectively, for five types of nanoparticles which are Cu, Ag, Al_2O_3, CuO, and TiO_2. He reported that the high Nusselt number inside the recirculation zone mainly depended on the thermophysical properties of the nanoparticles and it is independent of Reynolds number.

The study of steady laminar mixed convection flow over double forward-facing steps utilizing nanofluids in a two-dimensional horizontal configuration under uniform heat flux boundary conditions seems not to have been investigated in the past and this has motivated the present study. Thus, the present study deals with different types of nanofluids such as (Al_2O_3, CuO, SiO_2, and ZnO) with different volume fractions and different nanoparticle diameters. The effects of heat flux and Reynolds number on the velocity distribution, skin friction coefficient, and Nusselt number are studied and reported to illustrate the effect nanofluids on these parameters for flows.

Numerical Model

Physical Model

Considering the forward double facing steps placed in channel as shown in Figure (1) as a representation of a mixed convective flow. The wall downstream of the step (a) is maintained at a uniform wall heat flux (q_x), while the straight wall that forms the other side of the channel is maintained at constant temperature equivalent to the inlet fluid temperature (T_{in}). The wall downstream of the step (b, c) and the step it-self (h_1,h_2) are considered as adiabatic.

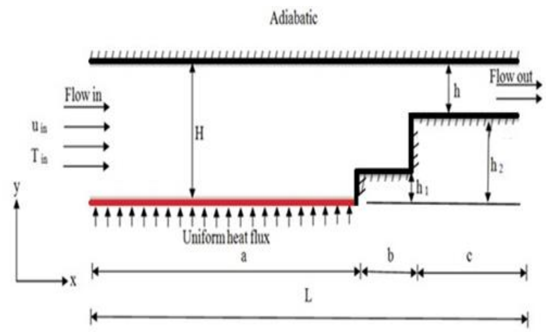

Fig.1. Schematic diagram for 2D FFS in a channel flow

Nanofluids at the channel entrance are considered to be hydrodynamically steady and the fully developed flow is attained at the edge of the step, and the streamwise gradients of all quantities at the channel exit where set to be zero.

This study exclusively deals with laminar flows. The nanoparticles and the base fluid (i.e. water) are assumed to have a thermal equilibrium and no slip condition occurs. The fluid flow is assumed to be Newtonian and incompressible. Flow radiation heat transfer and viscous dissipation term are neglected. The internal heat generation is not conducted in this study. The thermophysical properties of the nanofluids are constant and only affected by buoyancy force, which means that the body force acting on the fluid is the gravity, the density is varied and can be adequately modeled by the Boussinesq approximation. GAMBIT 2.4.6 and FLUENT 6.3, commercial software were used in the current study to perform the simulations [21].

$$\rho - \rho_\infty = (T - T_\infty) \qquad \ldots\ldots\ldots\ldots\ldots\ldots\ldots\ldots (1)$$

where, ρ is density, T is temperature, β is coefficient of thermal expansion, ρ_∞ and T_∞ are free stream density and temperature, respectively. Once these assumptions are made, it is possible to derive the governing equation of the nanofluids flow over a forward double step.

Governing Equations

To complete the CFD analysis of forward facing double steps, it is important to set up the governing equations (continuity, momentum, and energy). Using the Boussinesq approximation and neglecting the viscous dissipation effect governing equations for two dimensional laminar incompressible flows can be written as follows[20].

- The continuity equation

$$\frac{\partial u}{\partial x}+\frac{\partial v}{\partial y}=0 \quad \ldots\ldots\ldots\ldots\ldots\ldots\ldots\ldots\ldots(2)$$

- The x-momentum equation

$$u\frac{\partial u}{\partial x}+v\frac{\partial u}{\partial y}=-\frac{1}{(1-\varphi)+\varphi\frac{\rho s}{\rho f}}\frac{\partial p}{\partial x}+\frac{1}{\mathrm{Re}}\frac{1}{(1-\varphi)^{2.5}\left((1-\varphi)+\varphi\frac{\rho s}{\rho f}\right)}\left(\frac{\partial^2 u}{\partial x^2}+\frac{\partial^2 u}{\partial y^2}\right) \quad \ldots\ldots\ldots\ldots\ldots\ldots\ldots\ldots\ldots(3)$$

- The y-momentum equation

$$u\frac{\partial v}{\partial x}+v\frac{\partial v}{\partial y}=-\frac{1}{(1-\varphi)+\varphi\frac{\rho s}{\rho f}}\frac{\partial p}{\partial y}+\frac{1}{\mathrm{Re}}\frac{1}{(1-\varphi)^{2.5}\left((1-\varphi)+\varphi\frac{\rho s}{\rho f}\right)}*\,*\left(\frac{\partial^2 v}{\partial x^2}+\frac{\partial^2 v}{\partial y^2}\right) \quad \ldots\ldots\ldots\ldots\ldots\ldots\ldots\ldots\ldots(4)$$

- The energy equation

$$u\frac{\partial T}{\partial x}+v\frac{\partial T}{\partial y}=\frac{1}{\alpha}\left(\frac{\frac{k_{nf}}{k_f}}{(1-\varphi)+\varphi\frac{(\rho c_p)_s}{(\rho c_p)_f}}\right)\left(\frac{\partial^2 T}{\partial x^2}+\frac{\partial^2 T}{\partial y^2}\right) \quad \ldots\ldots\ldots\ldots\ldots\ldots\ldots\ldots\ldots(5)$$

Boundary Conditions

Laminar heat transfer problem considered in this paper is schematically shown in Figure (1). It is a channel with double FFS. The top wall and steps are insulated, whereas the bottom wall has heat flux which is hotter than the inlet flow temperature. Two-dimensional, steady-state, incompressible laminar flow is considered. The channel has double FFS which their height is h_1 and h_2, respectively. Height and length of the channel are depicted by H and L, respectively. Here, b and c show the length of steps, the length of bottom wall. The condition assumed at the inlet section are those of ambient condition (ambient temperature and velocity) while the only condition imposed at exit is uniform ambient pressure.

Code Validations and Grid Testing

Grid Independence Test

Grid independence tests were performed using different uniform grid densities to reach the most accurate results from the simulations. All the tests were carried out using air with Re number of 2000 at (T_{in}=20℃). Four mesh densities were examined (220 × 20), (240 × 30), (280×40) and (320 × 60). The uniform grid size of (280 × 40) confirms the grid independence test. Where it was found that, at the Nu corresponding to the grid density, when increase the number of intervals in both *y* and *x* direction does not affect significantly the value of Nusselt number. It shows less than 3% difference in Nusselt number compared with other grid sizes as shown in Figure (2). This observation indicates an adequate spatial resolution of the present simulation.

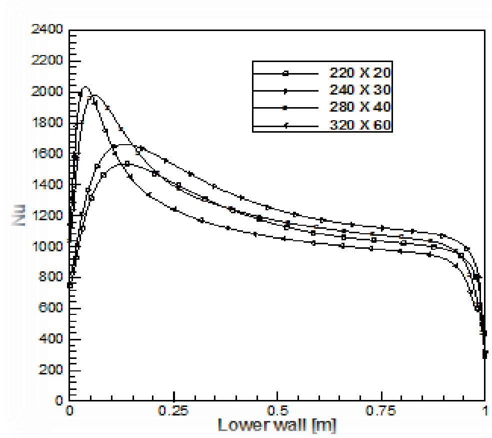

Fig.2. Grid independence test results

Code Validation

Code validation is very significant step in any numerical work in order to ensure that the numerical code is validated with other pervious works and it is ready for further runs. The present results obtained were compared and validated with the previous studies and acts as a benchmark for the project. On the other hand, it is not important only to get high accuracy of any numerical code but also to gain a better understanding on its capabilities and limitations.

Comparison was made in terms of Nusselt number, skin friction, and velocity distribution with results of Mohammed et al.[5] as can see in Figure (3). Mohammed et al. [5] used different types of nanofluids flow over backward facing step geometry which has adiabatic steps walls and heated bottom and upper walls. The comparison was carried out for (Re=225) and ($\Delta T=20^{\circ}C$) for diamonds nanofluids where laminar mixed convection flow was assumed. An excellent agreement was obtained between the present results and those of mentioned authors.

The 2nd validation of mixed convection flow is conducted with the results of Hong et al.[18].The Reynolds number is maintained constant at (Re=100) and uniform heat flux is fixed at (q_w=200W/m^2) for different inclination angles (0°, 90°, 135°, 180°, 315°). The results are validated and compared as shown in Figure (4).The present results indicate a good agreement with those of Hong et al. [18].

Numerical Parameters and Procedures

The numerical computation was carried out by solving the conservation equations along with the boundary conditions Equations (2) to (5). Equations for solid and fluid phase were simultaneously solved as a single domain. The discretization of governing equations in the fluid and solid regions was done using the finite-volume method (FVM). The diffusion term in the momentum and energy equations is approximated by second-order central difference which gives a stable solution. In addition, a second-order upwind differencing scheme is adopted for the convective terms. The numerical model was developed in the physical domain, and dimensionless parameters were calculated from the computed velocity and temperature distributions. The flow field was solved using the SIMPLE algorithm [22]. This is an iterative solution procedure where the computation is initialized by guessing the pressure field. Then, the momentum equation is solved to determine the velocity components. The pressure is updated using the continuity equation. Even though the continuity equation does not contain any pressure, it can be transformed easily into a pressure correction equation [23].

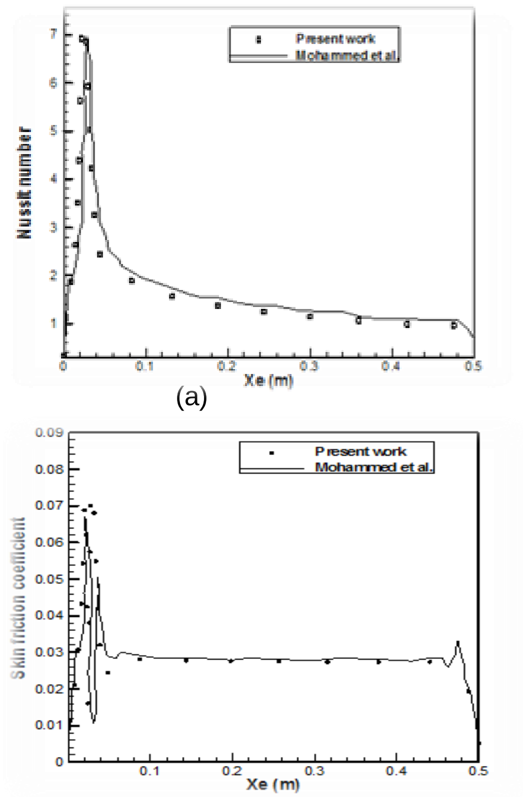

Fig.3. Comparison of the present results with the results of Mohammed et al. [5], (a) Nusselt number (b) Skin friction coefficient with Re= 225

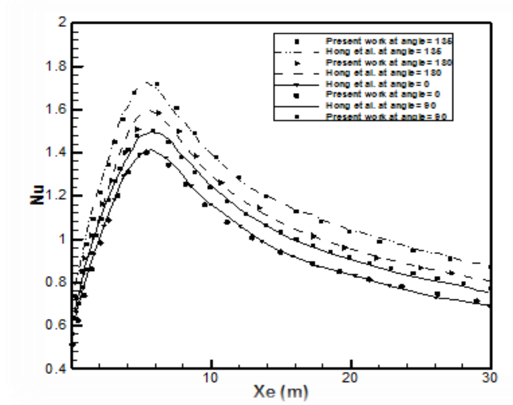

Fig.4. Comparison of Nusselt Number with the results of Hong et al. [18] (S=4.8 mm, and ER=2) for Re=100, and q_w=200 W/m^2 at different inclination angles

Thermophysical Properties of Nanofluids

In order to carry out simulations for nanofluids, the effective thermophysical properties of nanofluids must be calculated first. In this case, the nanoparticles being used, Al_2O_3, CuO, SiO_2 and ZnO. Basically the required properties for the simulations are effective thermal conductivity (k_{eff}), effective dynamic viscosity (μ_{eff}), effective mass density (ρ_{eff}), effective coefficient of thermal expansion (β_{eff}) and effective specific heat (cp_{eff}). Regarding these, the effective properties of mass density, specific heat and coefficient of thermal expansion are actually calculated according to the mixing theory.

- Effective Thermal Conductivity

By using the Brownian motion of nanoparticles forward and backward double steps, the effective the thermal conductivity can be obtained using the following mean empirical correlation [24]:

$$keff = k_{Static} + k_{Brownian} \quad \text{........................(6)}$$

Static Thermal Conductivity

$$k_{static} = k_{bf}\left[\frac{k_{np}+2k_{bf}-2(k_{bf}-k_{np})\emptyset}{k_{np}+2k_{bf}+(k_{bf}-k_{np})\emptyset}\right] \quad \text{.......... (7)}$$

Brownian Thermal Conductivity:

$$k_{Brownian} = 5\times10^4\,\beta\emptyset\rho_{bf}\,c_{p},bf\sqrt{\frac{kT}{2\rho_{np}}}.f(T,\emptyset) \quad \text{...(8)}$$

Where Boltzmann constant:

$k = 1.3807x10^{-23}\ J/K$

Modeling function, β [25]:

For Al_2O_3 $\beta = 8.4407(100\phi)^{-1.07304}$
$1\% \le \varphi \le 10\%$ 298 K ≤ T ≤ 363K

For CuO $\beta = 9.881(100\phi)^{-0.9446}$
$1\% \le \varphi \le 6\%$ 298 K ≤ T ≤ 363 K

For SiO_2 $\beta = 1.9526(100\phi)^{-1.4594}$
$1\% \le \varphi \le 10\%$ 298 K ≤ T ≤ 363K

For ZnO $\beta = 8.4407(100\phi)^{-1.07304}$
$1\% \le \varphi \le 7\%$ 298 K ≤ T ≤ 363 K

Modeling function, *f (T, Ø):*

$$f(T,\emptyset) = (2.8217\times10^{-2}\emptyset) + (3.917\times10^{-3})\left(\frac{T}{T_0}\right)$$
$$+(-3.0699\times10^{-2}\emptyset - 3.91123\times10^{-3})$$

- Effective Physical Properties

By using the Brownian motion of nanoparticles in over backward and forward double steps, the effective viscosity can be obtained as following mean empirical correlation [26]:

Viscosity:

$$\frac{\mu_{eff}}{\mu_f} = \frac{1}{1-34.87\left(\frac{d_p}{d_f}\right)^{-0.3}\emptyset^{1.03}} \quad \text{...................(9)}$$

Where:

Equivalent diameter of base fluid molecule:

$$d_f = \left[\frac{6M}{N\pi\rho_{bf}}\right]^{1/3} \quad \text{...........................(10)}$$

❖ where T is the temperature, Ø is the particle volume fraction, M is the molecular weight of the base fluid, N is the Avogadro number, f refers to nanofluid, bf refers to base fluid and p refers to nanoparticle.

❖ The density of the nanofluid ρ_{eff} [24]:

$$\rho_{nf} = (1-\emptyset)\rho_f + \emptyset\rho_{np} \quad \text{...................(11)}$$

where by ρ_f and ρ_{np} are the mass densities of the base fluid and the solid nanoparticles, respectively.

❖ The effective heat capacity at constant pressure of the nanofluid, $(\rho cp)_{nf}$ [24]:

$$(\rho c_p)nf = (1-\emptyset)(\rho c_p)f + \emptyset(\rho c_p)np \quad \text{......(12)}$$

when $(\rho_{c_p})_f$ and $(\rho c_p)_{np}$ are heat capacities of base fluid and nanoparticles, respectively.

❖ The effect coefficient of thermal expansion of nanofluid, $(\rho\beta)_{nf}$ [24]:

$$(\rho\beta)_{nf} = (1-\phi)(\rho\beta)_f + \phi(\rho\beta)_{np} \quad ......(13)$$

When $(\rho\beta)_f$ and $(\rho\beta)_{np}$ are thermal expansion coefficients of base fluid and nanoparticles, respectively.

Table 1. Thermophysical Properties for Pure Water, Different Nanofluids and different base fluids at T = 300K [24]

Thermophysical properties	Water	Al_2O_3	CuO	ZnO	SiO_2	Glycerin	Engine oil	Ethylene glycol
Density, ρ(kg/m³)	998.203	3970	6500	5600	2200	1259.9	884.1	1114.4
Dynamic viscosity, μ (Ns/m²)	2.01×10^{-3}	-	-	-	-	79.9	0.486	0.0152
Thermal conductivity, k (W/m.K)	0.613	40	20	13	1.2	0.286	0.145	0.252
Specific heat, cp (J/kg.K)	4182.2	765	535.6	495.2	703	2427	1909	2415
Coefficient of thermal expansion, β (1/K)	2.06×10^{-4}	5.8×10^{-6}	4.3×10^{-6}	4.3×10^{-6}	5.5×10^{-6}	4.8×10^{-6}	7×10^{-6}	6.5×10^{-6}

Results and Discussion

The Effect of Nanofluids Types

Nusselt Number

In this section, four different types of nanoparticles which are Al_2O_3, CuO, SiO_2 and ZnO and pure water as base fluid effects on the local Nusselt number over the bottom wall was presented. The Nusselt number for different nanofluids at Re = 1000, while volume fraction and particle diameter are 4% and 20 nm are shown in Figure (5). As can see similar trends of Nusselt number are obtained for all nanofluid. But in case of comparing among the four types of nanofluids, it is clear that the nanofluid with SiO_2 has the highest Nu number, followed by Al_2O_3, CuO and ZnO respectively. Nanofluids with higher Prandtl number have higher Nusselt number along the heated. Base fluid with SiO_2 nanoparticle has the highest Nusselt number values among the rest nanofluids, due to its highest thermal properties compared to the other nanofluids investigated, followed by Al_2O_3 then ZnO.

Skin Friction Coefficient

The skin friction coefficient of base fluid with different nanoparticles at Re = 1000 and the inlet T_{in} = 300K at the inlet, heat flux is q_w = 200 W/m^2 along the heated wall with nanoparticle size of 20 nm and volume fraction of 4% as shown in Figure (6). It is noticed that the skin friction is similar in the trend of local Nusselt number at that wall. Then, it slightly increases at near of duct's inlet section. After that, the skin friction coefficient decreases along the flow direction until it becomes minimum at the reattachment point where the velocity almost zero. This decrement caused by decreasing the dynamic pressure. It is shown that downstream the reattachment point, the skin friction coefficient increases until it reaches to another maximum. This peak occurs due to the recirculation flow where there is change in the velocity. After that the skin friction coefficient diminishes steeply until it reaches to the first step edge. The effect of skin friction coefficient for different nanofluids is insignificant and the difference is not clear because their results are much closed to each other [4].

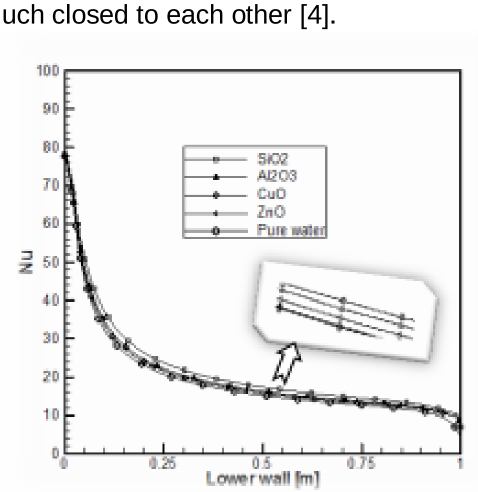

Fig. 5. Local Nusselt number for different nanofluids along the heated bottom wall Re=1000 with d_p=20 nm and ϕ = 4%.

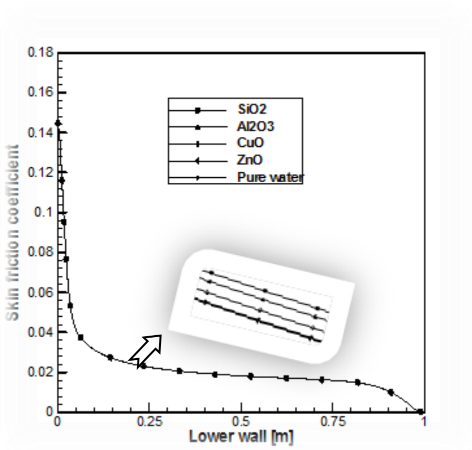

Fig. 6. Skin friction coefficient for different nanofluids along the heated bottom wall Re=1000 with d_p=20 nm and ɸ =4%

Velocity Distribution

The velocity distributions of different nanofluids with φ = 4% for Re=1000, d_p= 20 nm for different X/H sections along the down-stream wall is shown in Figure (7). It is clear from the figures at X/H = 1 and X/H = 30 that nanofluids with low density such as SiO_2 have higher velocity distribution at the edge of the baffle wall than those with high density such as CuO at constant Reynolds number. The flow is observed behind the step wall due to the recirculation region that attached to the step and the vortex which leaves the recirculation region and changes its direction down-stream the channel duo to the buoyancy force.

The Effect of Different Volume Fractions of Nanoparticles

The volume fraction of nanoparticles is actually referred to the volume of nanoparticles constituent divided by the volume of all constituents of the mixture prior to mixing. Volume fraction of nanofluids is the ratio of nanoparticles suspended in base fluids. Thus, pure water has zero volume fractions. In this study the volume fraction was in the range of 0 – 4% with Re = 1000 and nanoparticle diameter d_p=20 nm of (SiO_2) nanofluid is studied and Nusselt number for these condition is shown in Figure (9), and different volume fraction. Hence, nanofluids with higher volume fraction bring grater heat transfer enhancement. Because increasing the volume fraction leads to increase the thermal conductivity of the fluid.

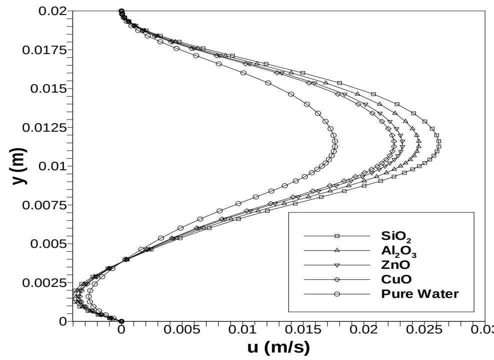

(a)

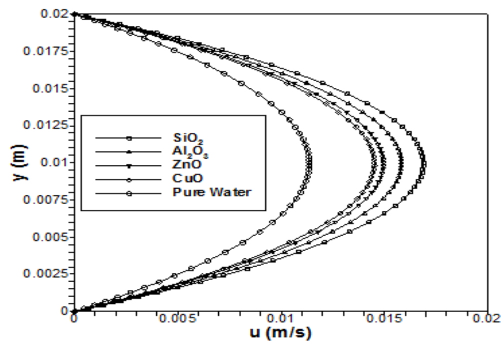

(b)

Fig. 7. Velocity distributions of different nanofluids with ɸ= 4% for Re=1000, d_p=20 nm and at (a) X/H = 9, (b) X/H = Exit

(a)

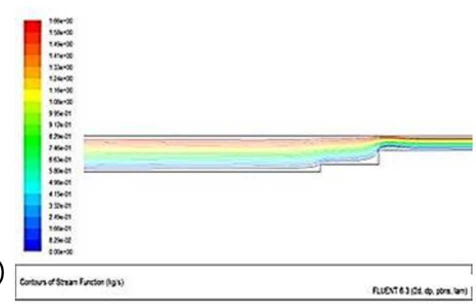

(b)

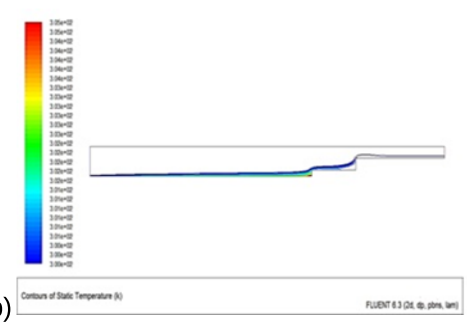

Fig. 8. (a) Streamlines and (b) isotherms for SiO_2 nanofluids flow with ɸ = 4% for Re = 1000, d_p =20 nm

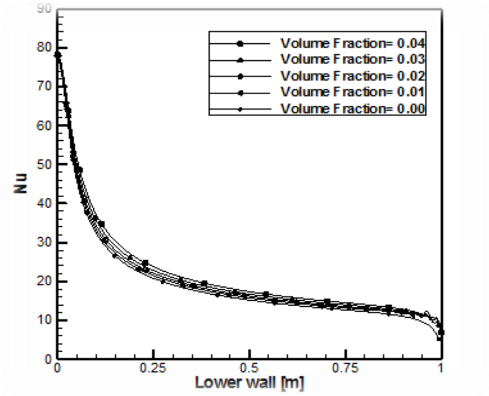

Fig.9. Local Nusselt number for different volume fractions along the heated bottom wall of SiO_2 nanofluids flow Re = 1000 at d_p = 20 nm

The Effect of Different Reynolds Numbers, Re

Nusselt Number

This study was done at Reynolds number in the range of 50-2000 laminar flow with volume fraction (∅=4%) and nanoparticles size d_p= 20 nm at horizontal position of SiO_2 nanofluid along the bottom heated wall is presented in Figure (10). At different values of Re, similar trends are obtained for the variation of Nu. As expected, increasing Re leads to increase the value of Nu along the heated lower wall.

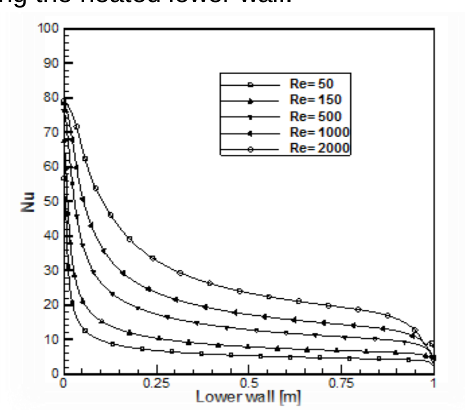

Fig. 10. Local Nusselt number along the heated bottom wall for different Reynolds numbers of SiO_2 nanofluid with laminar flow at ∅ = 4% and d_p = 20 nm

Skin Friction Coefficient

The skin friction of SiO_2 nanofluid with volume fraction (∅ = 4%), nanoparticle size (d_p = 20 nm) for different Reynolds numbers in the range of 50-2000 laminar flow at heat flux (q_w=200 W/m^2) along bottom wall is shown in Figure (11). It is observed that the skin friction decreases as Reynolds number increases. The trend of the skin friction coefficient is discussed in detail, previously. Therefore, as the velocity increases; the magnitude of Reynolds number increases and skin friction coefficient decreases. Because, the skin friction coefficient is inversely proportional to the velocity.

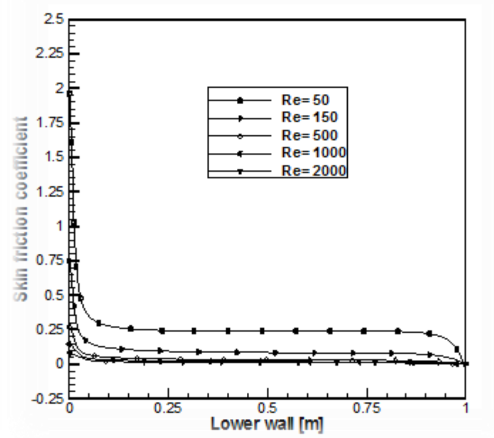

Fig. 11. Skin friction coefficient along the heated wall for different bottom wall for different Reynolds numbers of SiO_2 nanofluid with laminar flow at ∅ = 4% and d_p = 20 nm

Velocity Distribution

The velocity distribution for different Reynolds numbers ranged between 50 to 2000 of SiO_2 nanofluid with ∅=4%, q_w=200 W/m^{2}at bottom wall and d_p = 20 nm at different X/H is shown Figure (12). The velocity profile increases as Reynolds number increases. In addition, the size of all recirculation zones increases by increasing Re due to the increment in the velocity. Streamlines and isotherms are shown in Figure (13) which shows the development of these vortices.

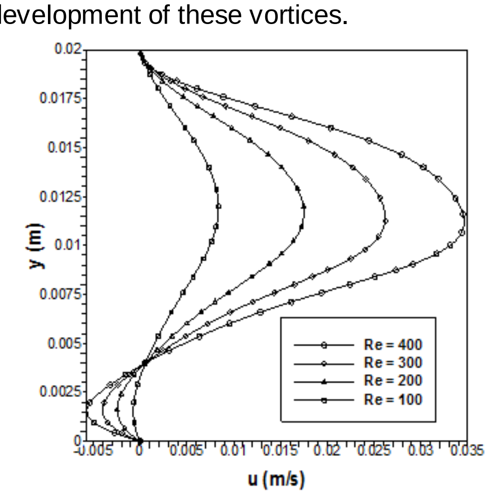

(a)

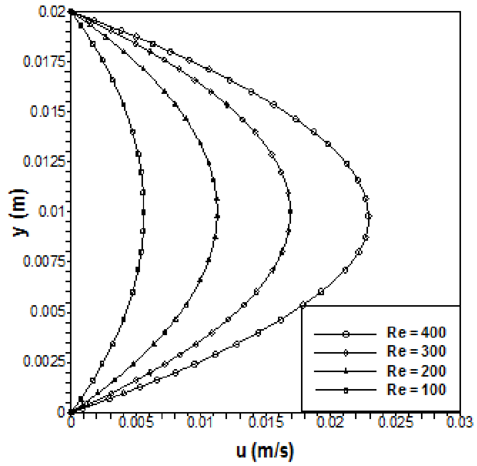

(b)

Fig. 12. Velocity distribution of SiO_2 nanofluid for different Reynolds number with ϕ = 4% and d_p = 20 nm at (a) X/H = 9, (b) X/H = Exit

(a)

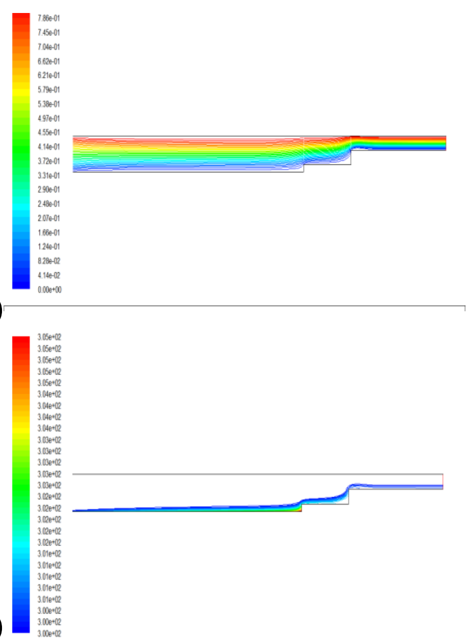

(b)

Fig. 13. Streamlines (a) and isotherms (b) for Re=2000 of SiO_2 nanofluids flow with ϕ = 4%, d_p = 20 nm

The Effect of Step Height

The effect of the two steps heights on Nusselt number distribution of SiO_2 nanofluid with $\varnothing$ = 4%, $q_w = 200$ W/m^2 in bottom wall and d_p = 20 at Re = 1000 and step heights in the range of 0.01m $\leq h_1 \leq$ 0.04m and 0.03m $\leq h_2 \leq$ 0.06m is presented in Figure14. It is shown that there is no considerable influence of the steps height on the Nusselt number. It is noted that the fact for high convective flow, importance effects move only from upstream, hence makes the space coordinate almost one way.

(a)

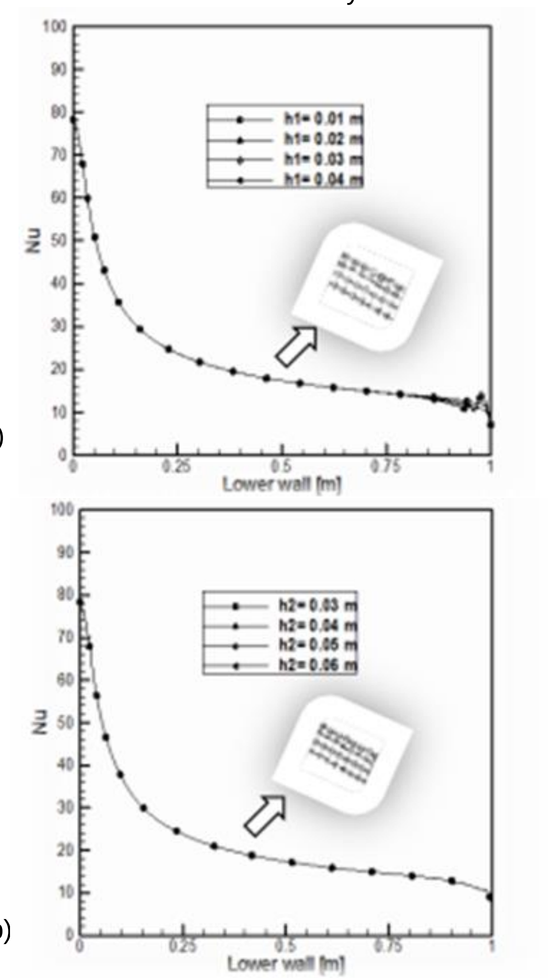

(b)

Fig. 14. Nusselt number for different steps heights of two steps (a) first step h_1, and (b) second step h_2 of SiO_2 nanofluid at Re = 1000

Conclusions

Numerical simulation of mixed convection heat transfer in inclined forward double steps using nanofluids was presented. The emphasis is given on the heat transfer enhancement resulting from various parameters, which include different nanofluids (Al_2O_3, CuO, SiO_2 and ZnO with base fluid (water), nanoparticles diameter in range of 20$\leq$ d_p $\leq$80nm, volume fraction (concentration) in the range of 0$\leq$ $\varnothing$ $\leq$4%, Reynolds number for laminar flow, Re in the range of 50 $\leq$ Re $\leq$ 2000, steps heights for forward double steps in the range of 0.01m $\leq h_1$ $\leq$0.04m, and 0.03m $\leq h_2 \leq$ 0.06m. The governing equations were solved using finite volume method with certain assumptions and appropriate boundary conditions to provide a clear understanding of the modeling aims and conditions for the present study.

It is found that the changing the types of nanoparticles, Al_2O_3, CuO, SiO_2 and ZnO, the results show that SiO_2 gives the highest Nusselt number followed by Al_2O_3, CuO and ZnO, respectively while pure water gives the lowest Nusselt number and the Nusselt number is found to increase with increasing the volume fraction of nanoparticles**.** The Nusselt number increased gradually when decreasing the nanoparticles diameter**.** It is found that there is no considerable influence of the steps height on the Nusselt number. The skin friction coefficient decreased with increasing Reynolds number and it has about same variation along the heated wall for different nanofluids, and The Nusselt number increased gradually by increasing the Reynolds number. The investigations of this work will surely solve many heat transfer related problems in the near future and are very likely to apply in the numerous practical heat transfer devices.

References

1. Griebl M, Dornseifer T, Neunhoeffer T. Numerical simulations in fluid dynamic. Philadephia: SIAM;1998.
2. Daungthongsuk W, Wongwises S. A critical review of convective heat transfer of nanofluids. Renewable and Sustainable Energy Reviews 2007;11(5):797-817.
3. Wang XQ, Mujumdar AS. Heat transfer characteristics of nanofluids: a review. International Journal of Thermal Sciences 2007;46(1):1-19.
4. Al-aswadi AA, Mohammed HA, Shuaib NH, Campo A. Laminar forced convection flow over a backward facing step using nanofluids. International Communications in Heat and Mass Transfer 2010;37(8):950-957.
5. Mohammed HA, Al-aswadi AA, Shuaib NH, Saidur R. Mixed convective flows over backward-facing step in a vertical duct using various nanofluids-buoyancy assisting case. In acceptance to Thermo Physics and Aeromechanics 2010; Springer, 2010.
6. Abu-Mulaweh HI, Armaly BF, Chen TS. Measurements in buoyancy-opposing laminar flow over a vertical forward-facing step. International Journal of Heat Mass Transfer 1996;39:1805-1813.
7. Abu-Mulaweh HI. Turbulent mixed convection flow over a forward-facing step-the effect of step heights. International Journal of Thermal Sciences 2005;44:155–162.
8. Abu-Mulaweh HI. Effects of backward- and forward-facing steps on turbulent natural convection flow along a vertical flat plate. International Journal Thermal Science 2002;41:376–385.
9. Abu-Mulaweh HI, Armaly BF, Chen TS. Measurements of laminar mixed convection in boundary-layer flow over horizontal and inclined backward-facing steps. International Journal of Heat Mass Transfer 1995;36:1883-1895.
10. Chiba K, Ishida R, Nakamura K. Mechanism for entry flow instability through a forward-facing step channel. Journal of Non-Newtonian Fluid Mechanical 1995;57:271- 282.
11. Hattori H, Nagano Y. Investigation of turbulent boundary layer over forward-facing step via direct numerical simulation. International Journal of Heat and Fluid Flow 2010;31:284–294.
12. Largeau JF, Moriniere V. Wall pressure fluctuations and topology in separated flows over a forward-facing step. Experimental Fluids 2007;40:42-21.
13. Yılmaz I, Öztop HF. Turbulence forced convection heat transfer over double forward facing step flow. International Communications in Heat and Mass Transfer 2006;33:508–517.
14. Dutta P, Dutta S. Effect of baffle size, perforation, and orientation on internal heat transfer enhancement. International Journal of Heat and Mass Transfer 1998;41(19): 3005-3013.
15. Yang YT, Hwang CZ. Calculation of turbulent flow and heat transfer in a porous-baffled channel. International Journal of Heat and Mass Transfer 2003;46(5): 771-780.
16. Nie JY, Hsieh H. Effects of a baffle on separated convection flow adjacent to backward-facing step. International Journal of Thermal Sciences 2009;48(3):618-625.
17. Lin JT, Armaly BF, Chen TS. Mixed convection heat transfer in inclined backward-facing step flows. International Journal of Heat and Mass Transfer 1991;34:1568-1571.

18. Hong B, Armaly, BF, Chen TS. Laminar mixed convection in a duct with a backward-facing step: the effects of inclination angle and Prandtl number. International Journal Heat Mass Transfer 1993;36:3059-3067.
19. Chiang TP, Sheu TWH, Tsai SF. Topological flow structures in backward-facing step channels. Computers & Fluids 1997;26:321-337.
20. Abu-Nada E. Application of nanofluids for heat transfer enhancement of separated flows encountered in a backward facing step. International Journal of Heat and Fluid Flow 2008;29(1):242-249.
21. Khanafer K, Vafai K, Lightstone M. Buoyancy-driven heat transfer enhancement in a two-dimensional enclosure utilizing nanofluids. International Journal of Heat and Mass Transfer 2003; 46:3639-3653.
22. Anderson JD. Computational fluid dynamics: the basics with applications. USA: McGraw-Hill; 1995.
23. Patankar SV. Numerical heat transfer and fluid flow. Hemisphere Publishing Corporation, Taylor and Francis Group; 1980.
24. Ghasemim B, Aminossadati SM. Brownian motion of nanoparticles in a triangular enclosure with natural convection. International Journal of Thermal Sciences 2010;49:931-940.
25. Vajjha RS, Das DK. Experimental determination of thermal conductivity of three nanofluids and development of new correlations. International Journal of Heat and Mass Transfer 2009;52(21-22):4675-4682.
26. Corcione M. Heat transfer features of buoyancy-driven nanofluids inside rectangular enclosures differentially heated at the sidewalls. International Journal of Thermal Sciences 2010;49:1536-1546.